

# JGR Atmospheres

## RESEARCH ARTICLE

10.1029/2021JD035016

### Key Points:

- High speed (down to submicrosecond time scales), high sensitivity lightning-like spectra (380–800 nm) reveal a rich chemistry
- Molecular species like CO, CN, C<sub>2</sub>, N<sub>2</sub>, and N<sub>2</sub><sup>+</sup> are detected. This opens the door to find and quantify lightning NO production by spectroscopy
- Electron concentrations and gas temperatures obtained from different methods are compared and discussed

### Correspondence to:

F. J. Gordillo-Vázquez,  
[vazquez@iaa.es](mailto:vazquez@iaa.es)

### Citation:

Kieu, N., Gordillo-Vázquez, F. J., Passas, M., Sánchez, J., & Pérez-Invernón, F. J. (2021). High-speed spectroscopy of lightning-like discharges: Evidence of molecular optical emissions. *Journal of Geophysical Research: Atmospheres*, 126, e2021JD035016. <https://doi.org/10.1029/2021JD035016>

Received 6 APR 2021

Accepted 20 MAY 2021

### Author Contributions:

**Conceptualization:** F. J.

Gordillo-Vázquez

**Data curation:** N. Kieu, M. Passas

**Formal analysis:** N. Kieu, F. J.

Gordillo-Vázquez

**Funding acquisition:** F. J.

Gordillo-Vázquez

**Investigation:** N. Kieu, F. J. Gordillo-

Vázquez, M. Passas, J. Sánchez, F. J.

Pérez-Invernón

**Methodology:** F. J. Gordillo-Vázquez,

M. Passas, F. J. Pérez-Invernón

**Project Administration:** F. J.

Gordillo-Vázquez

**Software:** N. Kieu, F. J. Pérez-Invernón

**Supervision:** F. J. Gordillo-Vázquez, M.

Passas, J. Sánchez

© 2021. The Authors.

This is an open access article under the terms of the [Creative Commons Attribution License](https://creativecommons.org/licenses/by/4.0/), which permits use, distribution and reproduction in any medium, provided the original work is properly cited.

## High-Speed Spectroscopy of Lightning-Like Discharges: Evidence of Molecular Optical Emissions

N. Kieu<sup>1</sup>, F. J. Gordillo-Vázquez<sup>1</sup> , M. Passas<sup>1</sup>, J. Sánchez<sup>1</sup>, and F. J. Pérez-Invernón<sup>2</sup>

<sup>1</sup>Instituto de Astrofísica de Andalucía (IAA), CSIC, Granada, Spain, <sup>2</sup>Deutsches Zentrum für Luft- und Raumfahrt, Institut für Physik der Atmosphäre, Oberpfaffenhofen, Germany

**Abstract** High speed spectra (between ~380 nm and ~800 nm) of meter-long lightning-like discharges recorded at 672,000 fps and 1,400,000 fps (with 1.488 and 0.714 μs time resolutions and 160 ns exposure time) show optical emissions of neutral hydrogen, singly ionized nitrogen, oxygen, and doubly ionized nitrogen which are similar to those found in natural lightning optical emissions. The spectra recorded in the near ultraviolet-blue range (380–450 nm) and visible-near infrared (475–793 nm) exhibited features of optical emissions corresponding to several molecular species (and emission bands) like cyanide radical (CN) (Violet bands), N<sub>2</sub> (Second Positive System), N<sub>2</sub><sup>+</sup> (first negative system), C<sub>2</sub> (Swan band) and CO (Quintet and Ångström bands). Molecular species can be formed at regions of the lightning-like channel where the gas temperature would be milder and/or in the corona sheath surrounding the heated channel. We have quantified and compared electron densities and temperatures derived from different sets of neutral and ion line emissions and have found different sensitivities depending on the lines used. Temperatures derived from ion emissions are higher and change faster than those derived from neutral emissions.

**Plain Language Summary** Lightning strokes are extremely fast atmospheric electricity events characterized by temperatures that can reach tens of thousands of degrees. Investigation of the fundamental properties of different types of lightning can help to deepen our understanding on lightning chemistry and, particularly, their contribution to key molecular gases such CO, CN, and NO, and also how different types of lightning propagate. High sensitivity, time-resolved optical emission spectroscopy is an ideal diagnostic technique to remotely study the fast temporal optical emissions of lightning. Our study explores the presence of molecular species production in heated lightning-like channels by using a forefront detector for microsecond and sub-microsecond time resolved lightning spectroscopy.

## 1. Introduction

Details of lightning spectroscopy studies in the first half of the twentieth century have been reviewed by Salanave (1961). Even though these early studies were on time-averaged spectroscopy over many lightning flashes, they already provided identification of some chemical species from their spectral features. Wallace (1960) examined a lightning spectrum in the near-ultraviolet (367–428 nm) that revealed the presence of the cyanide radical (CN) violet bands, N<sub>2</sub> second positive, and the N<sub>2</sub><sup>+</sup> first negative system (FNS) that allowed them to estimate rotational temperatures in the range 6,000–30,000 K (Wallace, 1960). Later, Wallace (1964) reexamined another lightning spectrum in a wider spectral region (315–980 nm) and identified more line emissions of singly ionized oxygen, nitrogen as well as the presence of Stark-broadened neutral oxygen and nitrogen lines. In the same period, Zhivlyuk and Mandel'shtam (1961) had also estimated gas temperatures in lightning that were around 20,000 K ± 5000 K.

Since the 1960s, time-resolved lightning spectroscopy has advanced, thanks to the development of new technologies for high speed recording. Salanave (1961) recorded the first time-resolved (averaged) lightning spectra using slitless spectroscopy techniques with time resolution of ~20 ns and spectral resolution of ~0.2 nm. The lightning spectra in the range 385–690 nm showed the presence of neutral, singly ionized ions of nitrogen, oxygen, and some emission features of CN and of the FNS of N<sub>2</sub><sup>+</sup>, but no doubly ionized species were detected. Stimulated by these initial lightning spectroscopic studies, a number of papers were soon afterward published on the use of lightning spectroscopy to investigate qualitative and quantitative properties of lightning Prueitt (1963); Uman (1963, 1964); Uman et al. (1964); Uman and Orville (1964, 1965);

**Validation:** J. Sánchez, F. J. Pérez-Invernón  
**Visualization:** N. Kieu  
**Writing – original draft:** F. J. Gordillo-Vázquez  
**Writing – review & editing:** F. J. Gordillo-Vázquez

Orville and Uman (1965). For instance, Prueitt (1963) calculated the excitation temperature of five different lightning strokes. Uman et al. (1964) studied the maximum possible values of the temperature, electron density, mass density of air and pressure in a lightning channel. They also discussed the continuum spectra, the opacity and the optical thickness in these papers. These quantitative analyses laid the foundation of lightning spectroscopic diagnostics.

Orville (1968a) recorded the first time-resolved spectra of cloud-to-ground lightning return strokes between a thundercloud and the ground. This was achieved by using slitless spectroscopy recorded on film with two high-speed streak cameras. These spectra were obtained in the 400–660 nm spectral range with time resolution of 2–5  $\mu\text{s}$  and 1 nm wavelength spectral resolution that allowed recording the optical emissions of neutral hydrogen, neutral and singly ionized atoms of nitrogen and oxygen. No molecular or doubly ionized emissions were identified. The temperature estimated from these strokes showed a rising trend in the first 10  $\mu\text{s}$  up to around 28,000–31,000 K and then decreased. The dynamics of electron density derived from the Stark-broadened  $\text{H}_\alpha$  exhibited a decreasing trend from  $\sim 10^{18} \text{ cm}^{-3}$  to  $\sim 10^{17} \text{ cm}^{-3}$  (Orville, 1968b).

Newman et al. (1967) were the first to produce triggered-lightning strokes using a rocket carrying aloft stainless steel wire to fire a potential thundercloud lightning. Later, in the 1980s and 1990s, a new generation of fast and sensitive camera sensors were introduced, thanks to the development of CCD and CMOS technology. This led to a new era of lightning and laboratory produced lightning-like discharges spectroscopy using high-speed cameras. During the summers of 2012 and 2013, Walker and Christian (2017) obtained the first high-speed spectra of triggered lightning at 672,000 fps (1.5  $\mu\text{s}$  of time resolution). These spectra covered different phases of a lightning flash including the initial stage, dart leader, return stroke, and continuing current. Spectra of return strokes showed emission features of neutral, singly, and doubly ionized nitrogen and oxygen atoms and neutral argon and hydrogen. It was the first time that doubly ionized nitrogen atoms were identified. However, no molecular species were detected in their triggered lightning spectra. Their estimations of the gas temperature and electron density in the lightning channel led to values that were far more higher than previous results: the measured temperatures exceeded  $\sim 40,000 \text{ K}$  and electron densities reached  $\sim 10^{19} \text{ cm}^{-3}$ , thanks to their high-speed recording and sensitivity (Walker & Christian, 2019).

Recently, Kieu et al. (2020) have explored spectral features of meter long lightning-like discharges in the submicrosecond time regime. They used an ultrafast spectrograph named GrAnada Lightning Ultrafast Spectrograph (GALIUS) Passas et al. (2019). These lightning-like discharges were recorded at 2,100,000 fps with time resolution of 0.416  $\mu\text{s}$  (160 ns exposure time) within a reduced spectral range (645–665 nm). The spectra showed the dynamics of neutral hydrogen and neutral, singly and doubly ionized nitrogen. Even though the measured peak currents of these lightning-like discharges were quite humble ( $\sim 3 \text{ kA}$ ) compared to peak currents in real lightning, the estimation of the temperature and electron density gave similar results: measured electron densities reached values of up to  $\sim 10^{18} \text{ cm}^{-3}$  and the temperatures were as high as  $\sim 32,000 \text{ K}$ . The analyses carried out in Kieu et al. (2020) also indicated a possible disruption of equilibrium behind the shock front in the very early times.

Contrary to optical spectra of Transient Luminous Events (TLEs), where molecular optical emissions dominate over neutral and ionic emissions (Gordillo-Vázquez & Pérez-Invernón, 2021; Gordillo-Vázquez et al., 2018; Hampton et al., 1996; Kanmae et al., 2007; Parra-Rojas et al., 2013, 2015; Passas et al., 2016; Pérez-Invernón et al., 2018), lightning spectra mostly exhibit the presence of neutral and ion lines. The presence of molecular emissions in lightning spectra is interesting, since it indicates the presence of mild temperature regions and/or the activity of streamers surrounding the heated lightning channel where molecules can exist and be electronically excited.

In this study, we focus on the time-resolved spectroscopy of several lightning-like discharges using GALIUS in different wide spectral regions: near ultraviolet-blue (380–450 nm), visible-near infrared (475–793 nm), and the near infrared (770–805 nm). Most molecular optical emissions were detected in the near ultraviolet-blue (380–450 nm) region. Spectra in the visible range exhibited features of doubly ionized nitrogen and molecular  $\text{C}_2$  emissions together with the strongest light emissions from singly ionized nitrogen at 500 nm. Submicrosecond time resolution (0.714  $\mu\text{s}$ ) was used to record spectra in the near-infrared where neutral oxygen triplet (777 and 795 nm) and singlet (715 nm) lines were distinctly detected from the early time. We calculated the temperature and electron density from these neutrals and compared them with the results

derived from other neutral ( $H_{\alpha}$  at 656.30 nm) and ion (N II at 648 and 661 nm) lines. A discussion on these results follows in the study.

## 2. Instrumentation and Experimental Setup

The results presented here have been obtained with an ultrafast and high spectral resolution (between 0.29 and 0.75 nm) spectrograph named GALIUS. GALIUS is a portable, ground-based spectrograph able to record spectra of natural/triggered or lightning-like discharges with submicrosecond time resolution. GALIUS can be set up with a total of 22 configurations made of combinations of 10 collector lenses (focus lengths ranging from 25 to 200 mm), two different collimator lenses in the UV and visible-NIR range (105 mm with F#4.5 and 50 mm with F#1.2) and four interchangeable volume-phase holographic (VPH) gratings for spectral ranges from the near ultraviolet (380 nm) to the near infrared (805 nm) and high-spectral resolution (0.29–0.75 nm depending on the grating used). More details about GALIUS and its configurations can be found elsewhere (Kieu et al., 2020; Passas et al., 2019).

For all spectra presented here, GALIUS was set up in slit mode ( $50 \mu\text{m} \times 3 \text{mm}$ ), using the high-speed FASTCAM SAZ camera, 12-bit ADC pixel depth constructed on a very high sensitivity (monochrome ISO 50000) CMOS sensor with sensor size of  $1,024 \times 1,024 \text{ } 20 \mu\text{m}$  square pixels. In the near-ultraviolet blue range, the camera was set up with two collimator lenses (105 and 50 mm) and collector lens 50 mm (F#1.5) controlled by the grism R1 with central wavelength in 357 nm, spectral resolution 0.29 nm and 2086 lines/mm. The recording speed in this configuration was 672,000 fps (160 ns exposure time) and the spectra was recorded in the range 380–450 nm. In the visible-near infrared range, GALIUS used two similar collimator lenses (50 mm, F#1.2) and a collector lens (50 mm, F#1.67 for long sparks). Spectra in this region were recorded at 672,000 fps (160 ns exposure time) using the grism R2 with central wavelength in 656.30 nm, spectral resolution 0.75 nm and 1,015 lines/mm. This was the widest spectral range recorded. The recorded images showed spectral emissions from 475 nm upto 793 nm. Finally, the camera was set up to allow submicrosecond time resolution in the near-infrared spectral range. These spectral images were obtained at 1,400,000 fps ( $0.714 \mu\text{s}$  time resolution and 160 ns exposure time) within the 770–805 nm spectral range. We used grism R4 with central wavelength in 778 nm, spectral resolution of 0.34 nm and 1,727 lines/mm. The collimator and collector lenses were the same as with the set up used with grism R2.

In 2019, we moved GALIUS to the facilities of the company DENA Desarrollos in Terrassa (Spain) to work with  $\sim 1\text{-m}$ -long lightning-like discharges produced by a 2.0 MV Marx generator. This generator can produce sparks up to 900 kV in Switching Impulse (SI) and Lightning Impulse (LI) modes. The experimental setup used here can be found elsewhere (Kieu et al., 2020). In the SI mode, the voltage slowly rises up to its maximum peak in  $100 \mu\text{s}$  and then it decays in  $\sim 0.5 \mu\text{s}$ . In the LI mode, the voltage rapidly reaches its peak in  $0.5 \mu\text{s}$ , keeping a plateau of  $2\text{--}3 \mu\text{s}$  and then decaying in  $0.5 \mu\text{s}$ . Opposite to voltage, the current in the SI mode reaches its peak and immediately decays, while the current in the LI mode rises up fast ( $0.3\text{--}0.5 \mu\text{s}$ ) but decays slowly in about  $100 \mu\text{s}$ . The LI mode is most similar to triggered and natural lightning where the current rise time is relatively fast (several  $\mu\text{s}$ ) and the current decays in tens to hundreds of  $\mu\text{s}$  (Walker & Christian, 2019). Natural lightning can exhibit peak currents much higher (15–150 kA) than the ones usually available in experimental facilities. In spite of this, we have obtained similar temperatures (and only slightly lower electron densities) than obtained in natural (Orville, 1968b) and triggered lightning (Walker & Christian, 2019).

In the following sections, we will show and discuss spectra of lightning-like discharges in the SI and LI modes produced with the same voltage (800 kV) and that generates  $\sim 1\text{-m}$ -long discharges  $\sim 8.5 \text{m}$  away from GALIUS.

## 3. GALIUS Time-Resolved Spectra

### 3.1. GALIUS Spectra in the Near Ultraviolet-Blue (380–450 nm)

Time-resolved spectra in the near-ultraviolet were recorded by grism R1 at 672,000 fps ( $1.488 \mu\text{s}$  time resolution) from 380 to 450 nm, as shown in Figure 1 for discharges generated in the LI mode. A zoom in of the spectral region between 400 and 425 nm is shown in Figure 1 (b). No spectra could be recorded in the

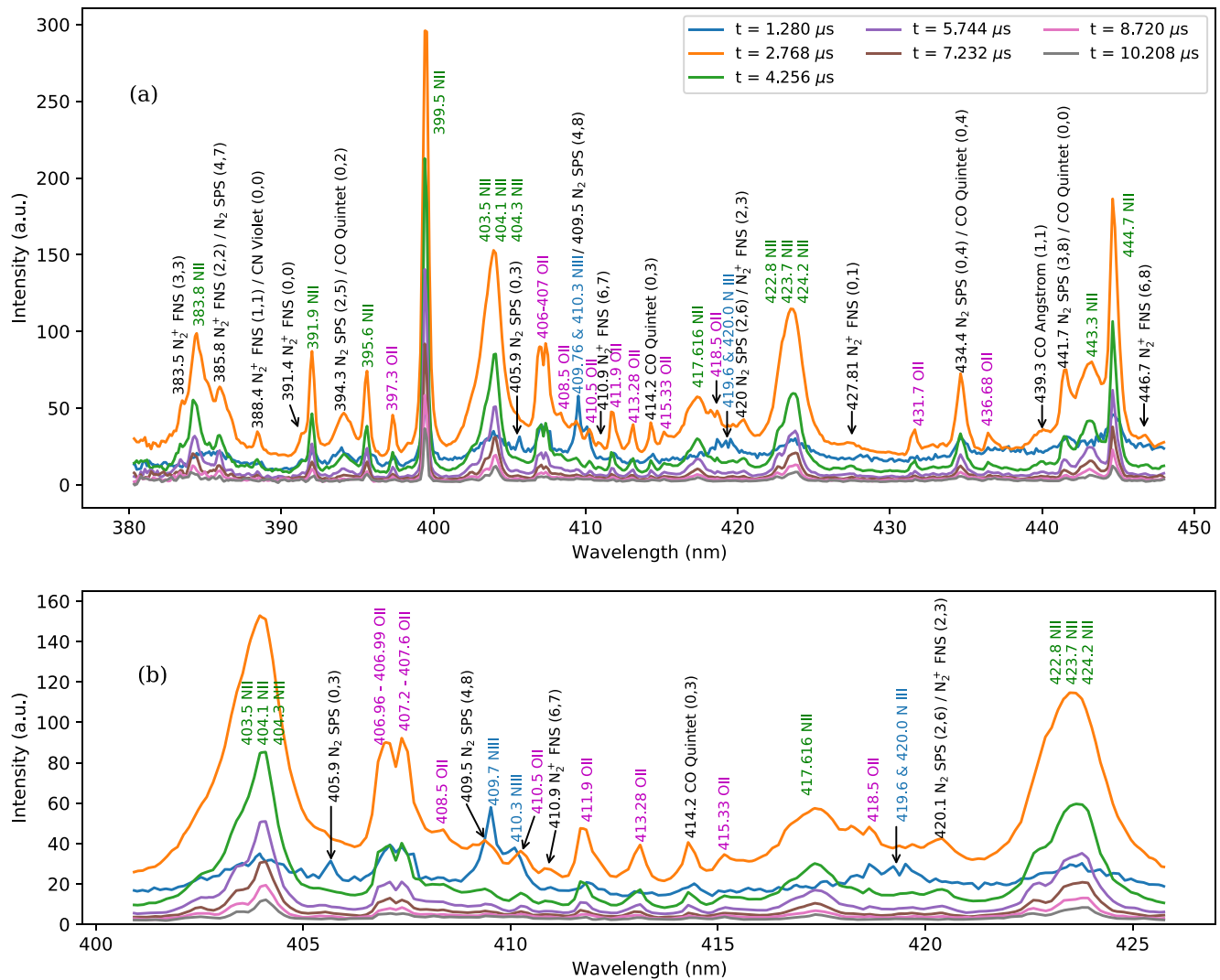


**Figure 1.** Time resolved R1 (380–450 nm) spectra of a meter long lightning-like discharge produced with the Lightning Impulse (LI) mode of a Marx generator with 800 kV. Panel (a) shows the entire spectral range. Panel (b) displays a zoom of the 400–425 spectral gap. The spectrum was recorded at 672,000 fps (160 ns exposure time) with spectral and time resolutions of 0.29 nm and 1.488  $\mu$ s, respectively. Spectral lines of singly ionized atomic nitrogen and oxygen, doubly ionized atomic nitrogen and several molecular species ( $N_2$ ,  $N_2^+$ ,  $C_2$ , CN, and CO) are visible and marked with green, purple, blue and black labels, respectively.

SI mode in this spectral region due to the faint luminosity and short life time of the discharge. To identify emitting species, we have labeled these spectra with their corresponding wavelengths and ionization states, for example, neutral nitrogen (N I), singly ionized nitrogen (N II), and doubly ionized nitrogen (N III).

Figure 1 shows the presence of singly ionized atomic nitrogen and oxygen, doubly ionized atomic nitrogen together and molecular optical emissions that were labeled in green, purple, blue and black color, respectively. The doubly ionized nitrogen lines at 409.7 nm, 410.3 nm were first reported by Walker and Christian (2017) but the 419.6 and 420.0 nm reported here were not seen before in this region. They only appear in the first frame (at 1.28  $\mu$ s) of the near-ultraviolet spectra. Many optical emissions in this near ultraviolet blue region are due to molecular species. Optical emissions of the CN violet band system ( $B^2\Sigma^+, v' \rightarrow X^2\Sigma^+, v''$ ) contributed with the presence of the line 388.3 nm ( $v' = 0 - v'' = 0$ ). The  $N_2$  second positive system (SPS) shows two transitions at 394.3 nm ( $v' = 2 - v'' = 5$ ) and 405.8 nm ( $v' = 0 - v'' = 3$ ) (Gordillo-Vázquez et al., 2012; Luque & Gordillo-Vázquez, 2011). The  $N_2^+$  FNS can be identified by humps at 388.4 nm ( $v' = 1 - v'' = 1$ ), 391.4 nm ( $v' = 0 - v'' = 0$ ) and 427.81 nm ( $v' = 0 - v'' = 1$ ). Some of these lines were earlier reported in lightning spectra (Salanave et al., 1962; Wallace, 1960). After these early molecular detections, there were no modern reports on molecular emissions in lightning spectra.

**Table 1**  
Molecular Species and Vibro-Electronic Optical Transitions Detected in the Present Study

Molecule	System name	Transition	Measured wavelength (nm) & vibrational transition ( $v_e', v_v'$ )
$N_2^+$	First negative	$B^2\Sigma_u^+ - X^2\Sigma_g^+$	383.54 (3,3), 385.79 (2,2), 388.43 (1,1), 391.44 (0,0), 410.90 (6,7), 420.00 (2,3), 427.81 (0,1), 446.66 (6,8)
$N_2$	Second positive	$C^3\Pi_u - B^3\Pi_g$	385.80 (4,7), 394.30 (2,5), 405.94 (0,3), 409.50 (4,8), 420.05 (2,6), 434.40 (0,4), 441.70 (3,8)
CO	Ångström system	$B^1\Sigma - A^1\Pi$	439.31 (1,1)
CO	Quintet states	$a''^5\Pi - d^3\Delta$	441.60 (0,0)
CO	Quintet states	$a''^5\Pi - a'^3\Sigma^+$	394.32 (0,2), 414.20 (0,3), 434.56 (0,4)
CN	Violet system	$B^2\Sigma^+ - X^2\Sigma^+$	388.30 (0,0)
$C_2$	Swan band	$d^3\Pi_g - a^3\Pi_u$	516.50 (0,0)

$N_2$  Second Positive System (SPS) and  $N_2^+$  first negative system (FNS) transitions were taken from “Camacho et al., 2007 and Gilmore et al., 1992”. Transitions of CO were taken from Czech et al. (2013) and Al-Tuwirqi et al. (2012). Transitions from  $C_2$  and CN were taken from Wallace (1960); Wallace (1964); and Czech et al. (2012).

Our R1 (near-ultraviolet blue) spectra includes the presence of traces of several CO optical emissions associated to the CO Ångström ( $B^1\Sigma, v' \rightarrow A^1\Pi, v''$ ) and Quintet systems ( $a''^5\Pi, v' \rightarrow a'^3\Sigma^+, v''$  and  $a''^5\Pi, v' \rightarrow d^3\Delta, v''$ ). In particular, we found the lines 394.32, 414.20, 434.56, 441.6, and 439.31 nm that belong to the (0, 2), (0, 3), (0, 4), (0, 0), and (1, 1) vibrational transitions of the Quintet and Ångström systems, respectively. In addition, three transitions associated to the CO Quintet system overlap with optical emissions of the  $N_2$  second positive system. Table 1 shows all the molecular transitions detected and displayed in Figure 1.

The presence of ground state and electronically excited CO in lightning-like discharges could be explained by the action of thermal dissociation of  $CO_2$  ( $CO_2 \rightarrow CO(X^1\Sigma_g, v \geq 0) + O(^3P)$ ), electron-impact dissociation of  $CO_2$  ( $CO_2 + e \rightarrow CO(X^1\Sigma_g, v \geq 0) + O(^3P) + e$ ),  $N + CO_2 \rightarrow NO + CO(X^1\Sigma_g, v \geq 0)$  and electron-impact excitation of ground state CO ( $CO(X^1\Sigma_g, v \geq 0) + e \rightarrow CO(B^1\Sigma, a''^5\Pi, a'^3\Sigma^+, v \geq 0) + e$ ) taking place in the shocked air surrounding the lightning-like channel, which is cooled rapidly by hydrodynamic expansion (Levine et al., 1979; Ripoll et al., 2014). This mechanism would prevent CO from further dissociation and could support the detection of CO (Levine et al., 1979). If, on the contrary, CO was produced in the slower-cooling inner core of the lightning channel, no CO would be produced (it would have been lost by thermal dissociation) and no CO would be detected (Levine et al., 1979). Once ground-state  $CO(X^1\Sigma_g)$  is produced, excited electronic states producing Ångström and Quintet states can be produced by thermal and/or electron-impact excitation.

It is interesting to note that although traces of CO are detected in the present spectroscopic analysis of lightning-like discharges as well as with chemical detectors in previous studies (Levine et al., 1979), global atmospheric chemistry circulation models predict that CO is slightly depleted by the action of lightning (Gordillo-Vázquez et al., 2019; Murray, 2016). A possible explanation for this could be that once CO is produced in the lightning channel, it is depleted by reactions involving lightning produced OH and ground state oxygen atoms  $O(^3P)$  like  $CO + OH \rightarrow CO_2 + H$ ,  $CO + OH + O(^3P) \rightarrow CO_2 + OH$  and  $CO + OH + O_2 \rightarrow CO_2 + HO_2$ .

The detection of  $C_2$  and, in particular, the formation of  $C_2(d^3\Pi_g, v)$  underlying the Swan band optical emissions can be explained in terms of the presence of  $CO(X^1\Sigma_g, v)$  in the lightning-like channel. At relatively high temperatures (4000–6000 K) typical of air in the edge of the expanding channel of a lightning-like discharge, ground state  $C(^3P)$  atoms can be efficiently produced through the reaction  $CO(X^1\Sigma_g, v_1) + CO(X^1\Sigma_g, v_2) \rightarrow CO_2 + C(^3P)$  (Carbone et al., 2020). Once  $C(^3P)$  is formed, Little and Browne (1987) proposed a possible three step mechanism for the formation of  $C_2(d^3\Pi_g, v)$  producing the Swan band through: (a)  $C(^3P) + C(^3P) + M \rightarrow C_2(^5\Pi_g, v) + M$ , (b)  $C_2(^5\Pi_g, v) + M \rightarrow C_2(^5\Pi_g, v = 0) + M$  and (c)  $C_2(^5\Pi_g, v = 0) + M \rightarrow C_2(d^3\Pi_g, v = 6) + M$ , where  $^5\Pi_g$  is a metastable (quintet) state for which a crossing exists between the  $v = 6$  level of the  $d^3\Pi_g$  and the  $v = 0$  of the  $^5\Pi_g$  state (Carbone et al., 2020).

The presence of CN and its violet band (due to the radiative deexcitation of  $CN(B^2\Sigma^+)$ ) in the R1 spectra can be explained by competing mechanisms for the formation of  $C_2$  and CN that promote and go in favor

of the formation of CN in aN<sub>2</sub> rich environment like air. According to Dong et al. (2014), once atomic carbon and molecular C<sub>2</sub> are available, CN radicals can be formed by C(<sup>3</sup>P) + N<sub>2</sub> → CN(X<sup>2</sup>Σ<sup>+</sup>) + N, C(<sup>3</sup>P) + N → CN(X<sup>2</sup>Σ<sup>+</sup>) and C<sub>2</sub> + N<sub>2</sub> → 2 CN(X<sup>2</sup>Σ<sup>+</sup>), C<sub>2</sub> + 2 N → 2 CN(X<sup>2</sup>Σ<sup>+</sup>). The excitation energy of CN(B<sup>2</sup>Σ<sup>+</sup>) is about 3 eV so that it can be easily produced by thermal and/or electron-impact excitation of ground state CN(X<sup>2</sup>Σ<sup>+</sup>) in the lightning-like channel. Alternative kinetic mechanisms for the formation of CN(X<sup>2</sup>Σ<sup>+</sup>) and CN(B<sup>2</sup>Σ<sup>+</sup>) would require the presence of the metastable N<sub>2</sub>(A<sup>3</sup>Σ<sub>u</sub><sup>+</sup>) through CO(X<sup>1</sup>Σ<sub>g</sub>) + N<sub>2</sub>(A<sup>3</sup>Σ<sub>u</sub><sup>+</sup>) → CN(X<sup>2</sup>Σ<sup>+</sup>) + NO and CN(X<sup>2</sup>Σ<sup>+</sup>) + N<sub>2</sub>(A<sup>3</sup>Σ<sub>u</sub><sup>+</sup>) → CN(B<sup>2</sup>Σ<sup>+</sup>) + N<sub>2</sub> (Crispim et al., 2021). These reaction paths should also be possible in mild temperature regions of the lightning-like channel so that ground state N<sub>2</sub> can be excited by electron collisions before dissociation occurs.

Figure 2 shows the fit of synthetic spectra of heated humid (80% relative humidity [RH]) air to the measured R1 spectra (normalized with respect to the 399.5 nm N II ion line) corresponding to the early times (from 1.28 μs to ~10.20 μs) of a meter-long LI discharge. As time increases, the measured gas temperatures decrease. The synthetic spectra are based on equilibrium calculations of thermal air plasmas (see supplementary material of Kieu et al., 2020). Calculated spectra include all possible lines of atoms, singly and doubly ionized ions that can appear in the R1, R2, and R4 spectral ranges explored in this study and considered in Kramida et al. (2020). The only molecular species considered is N<sub>2</sub> and, in particular, the Lyman-Birge-Hopfield (LBH) band, First Positive System (FPS), and Second Positive System (SPS). Stark broadening of nonhydrogenic (Bekefi, 1976) and hydrogenic lines (Griem, 1964) are included and convolved with instrumental broadening (0.29 nm for R1 and 0.75 nm for R2) using the measured electron densities and gas temperatures. Since no electron densities could be measured in the near ultraviolet-blue spectral range using grism R1, we used the electron concentrations measured with grism R3 (see panel [b] in Figure 6) in our previous paper since the spectral resolutions of R1 and R3 are similar (Kieu et al., 2020). From the measured R1 gas temperatures (see panel [d] in Figure 6), the corresponding equilibrium concentrations and partition functions of chemical species (atoms, ions and molecules) were calculated to generate the synthetic spectra.

The agreement between synthetic and measured R1 spectra is fine except for some N II ion lines (383.8, 403.5, 404.1, 404.3, 417.6, 422.8 nm, 423.7, and 424.2 nm), which predicted intensities are below the measured values and a few transitions of CO and of the N<sub>2</sub><sup>+</sup> FNS not included in the synthetic spectra calculation. Since the measured R1 spectra mostly include ionic emissions, their intensity rapidly decreases as the gas temperature evolves toward lower values. For instance, the strong N II ion lines at 399.5 and 444.7 nm fade away as time evolves.

The use of simulated spectra is justified because they contribute to detect the limits of our knowledge (accuracy of available spectroscopic constants and calculated Stark broadening mechanisms) and model approximations (equilibrium assumptions).

### 3.2. GALIUS Spectra in the Visible-Near Infrared (475–793 nm)

Time-resolved spectra in the visible-near infrared range from 475 to 793 nm were recorded with grism R2 at 672,000 fps as shown in Figures 3a and 3b, 3c for ~1 m-long, 800 kV discharges in SI and LI modes, respectively. We can see in the first frame (at  $t = 0.930 \mu\text{s}$  [SI mode] and  $t = 1.250 \mu\text{s}$  [LI mode], see panel [b]) of both figures the sharp rising of the singly ionized nitrogen (N II) at 500 nm. Then, in the second frame (at  $t = 2.418 \mu\text{s}$  [SI mode] and  $t = 2.738 \mu\text{s}$  [LI mode], see panel [b]), the 500 nm ion line reaches its maximum intensity. Similarly, Figure 3 also shows the evolution dynamics of the 777 nm neutral oxygen line with its rising from the first frame to its maximum at later times of around ~2.418 μs and ~8–10 μs for the SI and LI modes, respectively. The maximum intensity of the 500 nm N II line is much larger than the peak of the 777 nm O I line in these early times. However, the neutral 777 nm O I line lasts much longer (see panel [c]) than the singly ionized 500 nm N II line. The explanation for this is that ion emissions appear in the early time and remain excited only for a short time (a few microseconds) while the neutral emissions appear later but last much longer since they are easier to excite.

The second interesting feature in the R2 spectra of Figure 3 is the presence of a line at ~517 nm. This line was first identified by Orville (1968a) in an attempt to prove the existence of singly ionized oxygen lines in lightning spectra. However, when Orville (1968a) used it to calculate temperatures, the result

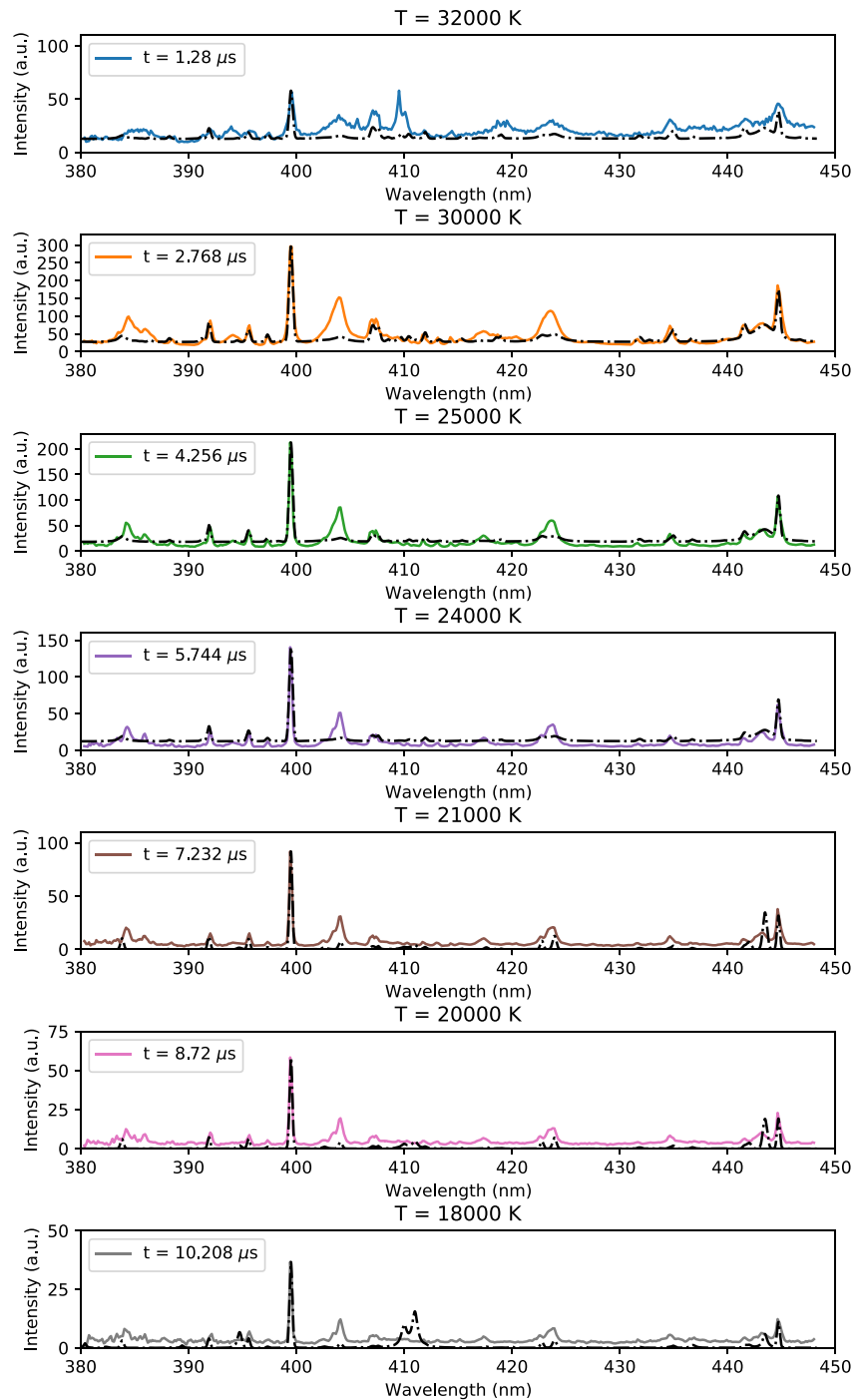


**Figure 2.** Comparison between calculated synthetic spectra (black dashed dotted line) of heated humid (80% RH) air and measured R1 (380–450 nm) spectra (color line) of a meter long Lightning Impulse (LI) discharge produced with a peak voltage of 800 kV. Note that synthetic spectra do not include molecular species except for the Lyman Birge Hopfield (LBH), Second Positive System (SPS) and First Positive System (FPS) bands of  $N_2$ .

yielded too high values in the range 40,000–70,000 K which considerably exceeded the temperature values 20,000–30,000 K previously derived by the same authors (Orville, 1968b). The singly ionized oxygen line at 517.5 nm seems to be a weak one (Kramida et al., 2020). This means that the line in this position of the R2 spectra may result from the overlapping of that oxygen ion line and another emission lines from other species. In particular, the  $C_2$  emission at 516.5 nm corresponds to the band head (0-0) which is the

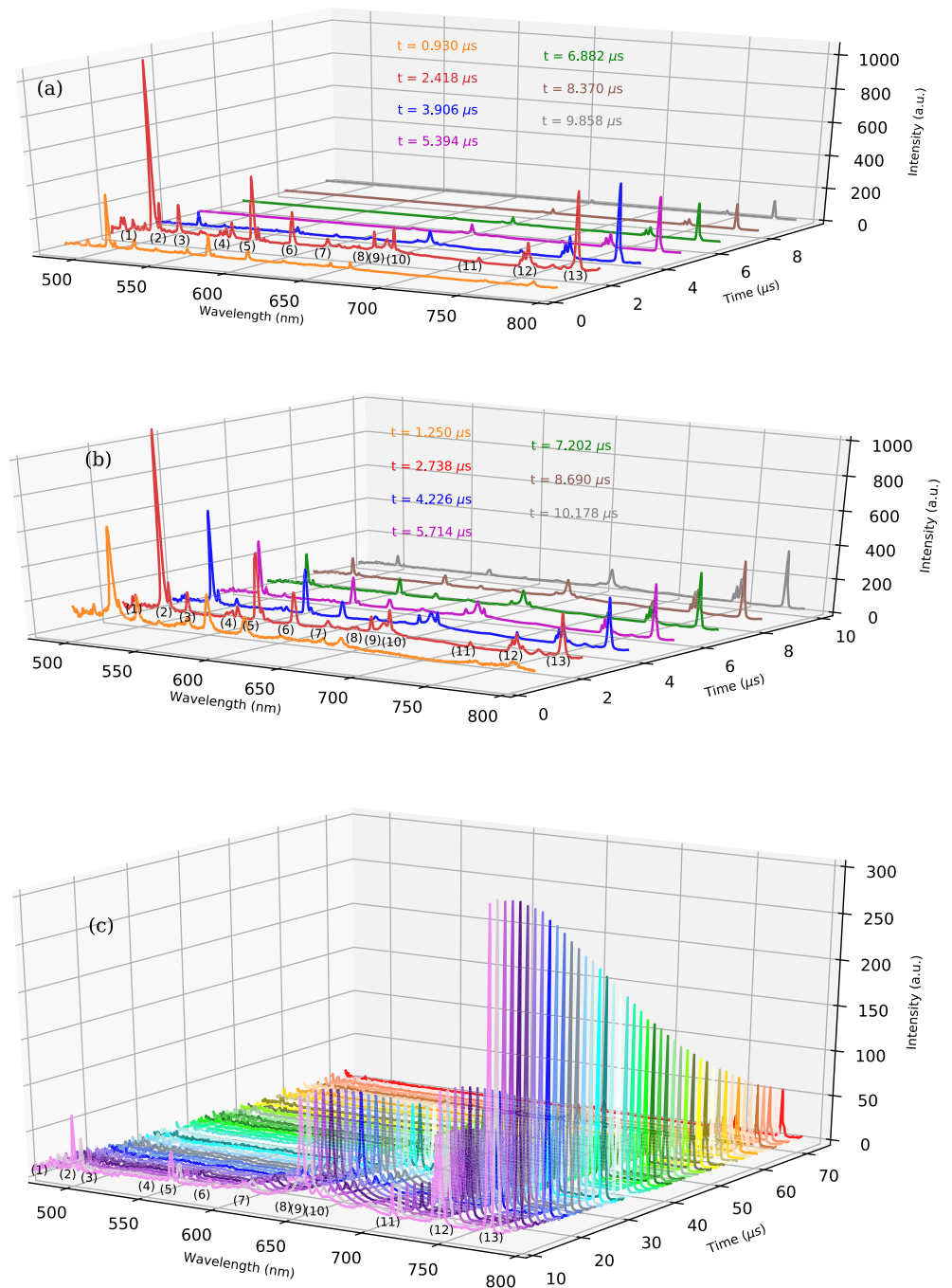


**Figure 3.** Time resolved R2 (475–793 nm) spectra of a meter long lightning-like discharge produced with the Switching Impulse (SI) mode (panel [a]) and Lightning Impulse (LI) mode (panels [b] and [c]) of a Marx generator with 800 kV. For easier comparison between SI and LI mode spectra, panels (a) and (b) show similar time range (but not exactly the same). Panel (c) for LI mode show spectra for times starting in 10.178  $\mu\text{s}$ . The spectra were recorded at 672,000 fps (160 ns exposure time) with spectral and time resolutions of 0.75 nm and 1.488  $\mu\text{s}$ , respectively. Spectral lines of neutrals (O I, N I, H I), singly ionized atoms (N II, O II) and the  $\text{C}_2$  Swan band head at 516.5 nm are visible. Note that the numbers stand for: (1) 485.8–486.7 N II, (2) 500.1–500.5 nm N II, (3) 516.5 nm  $\text{C}_2/\text{O II}$ , (4) 553.5 nm N II, (5) 567.9–571.0 N II, (6) 592.7–594.1 N II, (7) 616.8 nm N II, (8) 648.2 nm N II, (9) 656.3 nm H I, (10) 661.0 N II, (11) 715.6 O I, (12) 742.4–744.3–746.8 nm N I, (13) 777.4 nm O I.

strongest transition in the C<sub>2</sub> Swan band system (see Section 3.1). Therefore, it could be very possible that the recorded emission at ~517 nm corresponds to the overlapping of the C<sub>2</sub> (0-0) 516.5 Swan band and the singly ionized oxygen at 517.5 nm that could not be well resolved because of the limited spectral resolution (0.75 nm) of the R2 spectra.

Finally, other interesting line emissions present in the R2 spectra are those of several doubly ionized nitrogen at 485.8, 486.7, 532.0, and 532.7 nm in early times (from 0.93  $\mu$ s to ~2  $\mu$ s). These ion lines were recently identified in triggered lightning return stroke spectra recorded at 672,000 fps (Walker & Christian, 2017). However, in their identification the doubly ionized nitrogen lines were only present in the first frame of their spectra.

Figure 4 shows the fit of synthetic spectra of heated humid (80% RH) air to the measured R2 spectra (normalized with respect to the 500 nm N II ion line) corresponding to the early times (from 1.250  $\mu$ s to ~10.178  $\mu$ s) of a meter-long LI discharge. In a time gap of ~9  $\mu$ s the measured gas temperatures decrease from ~34,000 K to ~17,000 K as derived from the ratio of the 648 and 661 nm N II ion lines (see Figure 6e). The R2 synthetic spectra were calculated using as inputs the measured R2 electron densities (obtained from the H $\alpha$  line) and gas temperatures (see Figure 6). From the measured gas temperatures, the corresponding equilibrium concentrations and partition functions of chemical species (atoms, ions and molecules) were calculated to generate the corresponding R2 synthetic spectra.

There is a reasonable agreement between synthetic and measured R2 spectra except for the 656.30 nm H $\alpha$  line and the 567.9 nm line of the N II ion, which predicted intensities are below the measured values. The 777 nm line of O I is not well matched at 2.738  $\mu$ s. On the other hand, the C<sub>2</sub> Swan band peak at 516.5 nm was not included in the synthetic spectra calculation and so there is no synthetic line able to match that peak.

### 3.3. GALIUS Spectra in the Near-Infrared (770–805 nm)

In the near-infrared spectral region we focus the study on the dynamics of two neutral oxygen triplet lines at 777 and 795 nm. Their spectra were recorded at 1,400,000 fps with submicrosecond time resolution (0.714  $\mu$ s and 160 ns exposure time) as shown in Figure 5. The spectra recorded in this spectral range did not exhibit any molecular emissions. Figures 5a, 5b and 5c, 5d show the optical emissions from ~1-m-long spark produced with 800 kV in the SI and LI modes, respectively. The neutral O I line at 777 nm is in reality a triplet with sublines at 777.19, 777.42, and 777.54 nm. The O I line at 795 nm is also the combination of three lines at 794.75, 795.08, and 795.21 nm. These two triplet O I lines are among the longest lasting emission lines in lightning spectra, around 25  $\mu$ s in the SI mode and about 100  $\mu$ s following the duration of the input current of the LI mode. Neutral emissions usually appear a bit later but last longer than ion lines (Kieu et al., 2020; Walker & Christian, 2019). In spite of this, the emergence of the 777 nm line can be seen in a time as early as 0.25  $\mu$ s in the SI mode (see Figure 5b) and ~0.55  $\mu$ s in the LI mode (see Figure 5d). The emergence of the 795 nm line is weaker than the 777 nm one because, though they have very similar Einstein coefficients, the excitation energy of the 795 nm triplet is higher (~14.04 eV) than that of the 777 nm triplet (~10.73 eV). It is interesting to note that, as it is seen from high speed photometric recordings from space, lightning 777 nm optical radiation inside thunderclouds has a duration of several milliseconds due to scattering by water and/or ice particles before it is finally absorbed (Luque et al., 2020; Soler et al., 2020). Lightning near-infrared optical emissions inside thunderclouds are more absorbed than near-ultraviolet and blue radiation (Luque et al., 2020).

The nonscattered (by clouds) lightning 777 nm optical emission (mainly connected to the heated channel luminosity) is of interest for diagnostic purposes since its temporal dynamics closely follows that of lightning currents (Cummer et al., 2006; Fisher et al., 1993; Kolmašová et al., 2021; Walker & Christian, 2019). It is also tightly correlated to the distant quasi-static ( $\leq$ 0.1–400 Hz) magnetic field signature attributed to lightning continuum currents that have been associated to delayed sprites (Cummer & Füllekrug, 2001; Cummer et al., 2006). Recent results by Kolmašová et al. (2021) have demonstrated that, in addition to high-peak current of causative lightning strokes, the velocity of the current wave and the conductivity of the heated channel of the return stroke are important factors that control the intensity of elves. Cho and Rycroft (1998) had previously shown that the amplitude and the rise time of lightning affect the intensity of

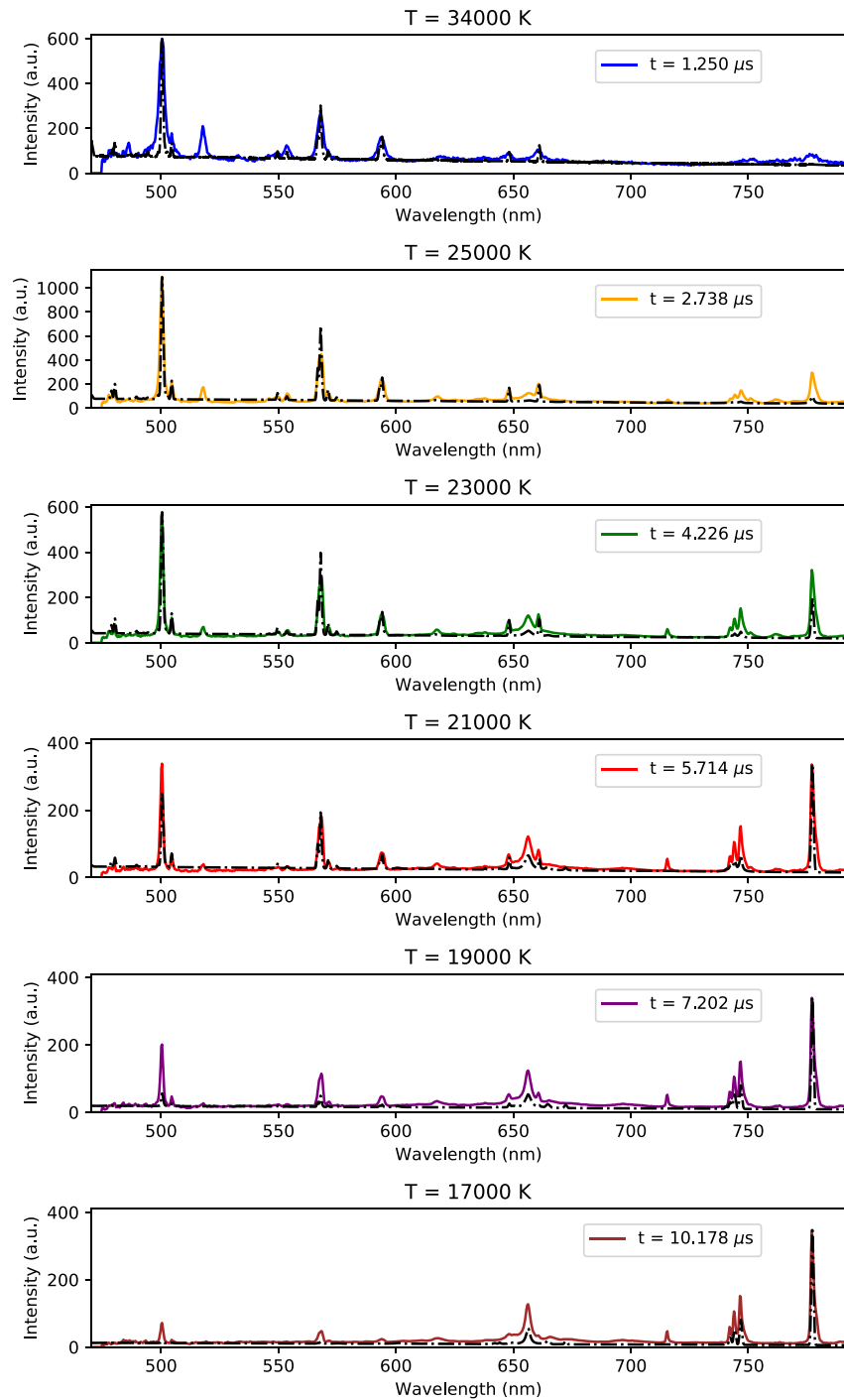


**Figure 4.** Comparison between calculated synthetic spectra (black dashed dotted line) of heated humid (80% RH) air and measured R2 (475–793 nm) spectra (color line) of a meter long Lightning Impulse (LI) discharge produced with a peak voltage of 800 kV. Note that synthetic spectra do not include molecular species except for the Lyman Birge Hopfield (LBH), Second Positive System (SPS) and First Positive System (FPS) bands of  $N_2$ . The peak associated to the  $C_2$  Swan band is visible at 516.5 nm.

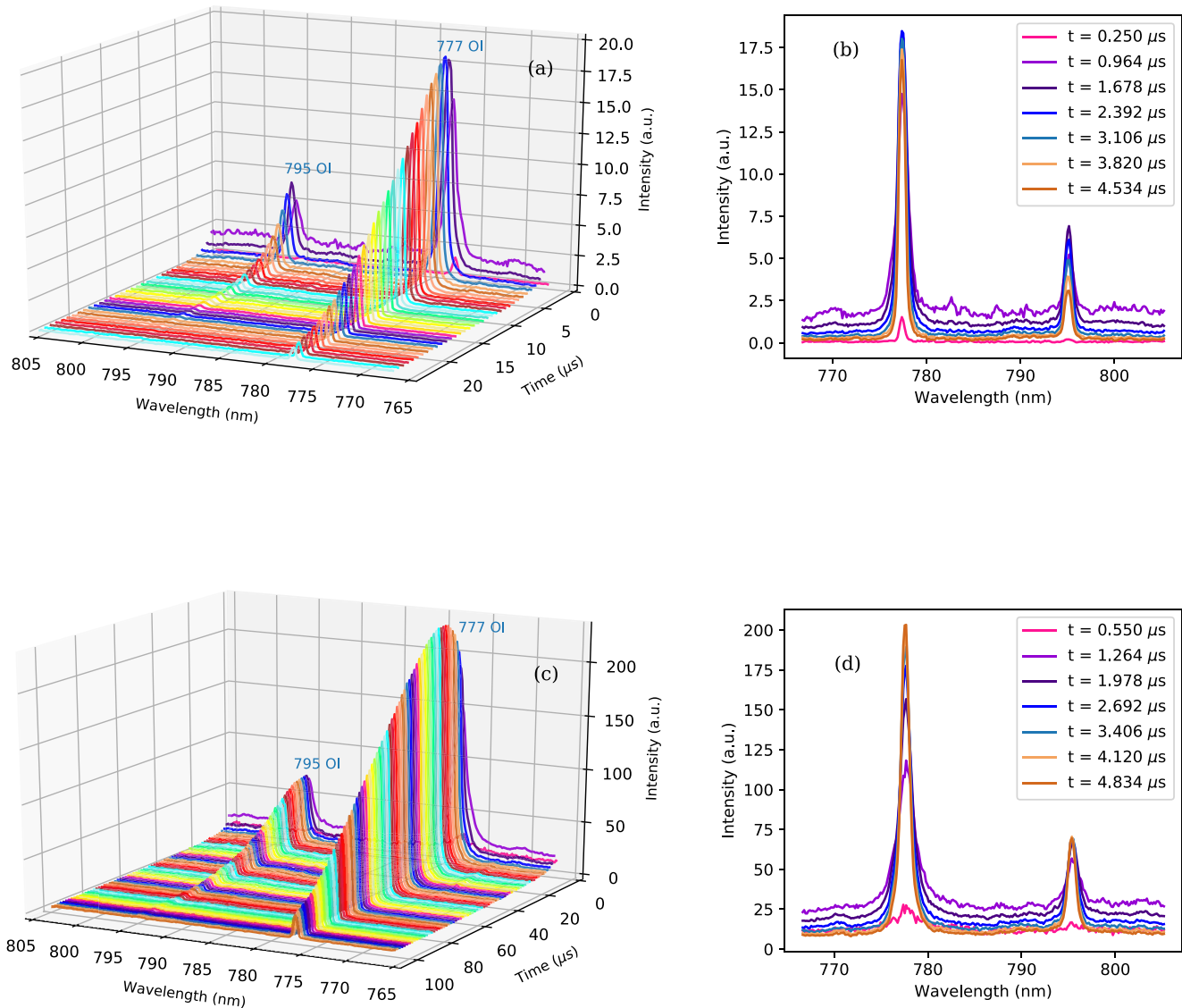


**Figure 5.** Time resolved R4 (770–805 nm) spectra of a meter long lightning-like discharge produced with the Switching Impulse (SI) mode (panels [a, b]) and Lightning Impulse (LI) mode (panels [c, d]) of a Marx generator with 800 kV. The spectra were recorded at 1,400,000 fps (160 ns exposure time) with spectral and time resolutions of 0.34 nm and 0.714  $\mu\text{s}$ , respectively. Triplets of oxygen neutrals (O I) at 777 and 795 nm are clearly visible.

elves. The amplitude relates to the lightning channel conductivity and the rise time influences the current wave velocity of the lightning return stroke pulse.

The electrical conductivity of the (heated) lightning channel can be affected by the ambient relative humidity which depends on season, environment, that is, coastal, maritime or inland, and regional climate. For instance, in high-altitude plateaus, the conductivity can be up to 20%–40% lower (Guo et al., 2009). We have explored the temporal dynamics of the electrical conductivity in a spot of the heated, highly ionized lightning-like channel.

#### 4. Quantitative Analysis: Electron Density, Temperature, and Conductivity

##### 4.1. Electron Density

Stark broadening is often used to estimate the electron density in lightning discharges (Orville, 1968b; Uman et al., 1964; Walker & Christian, 2019). The advantage of this method is that Stark broadening is

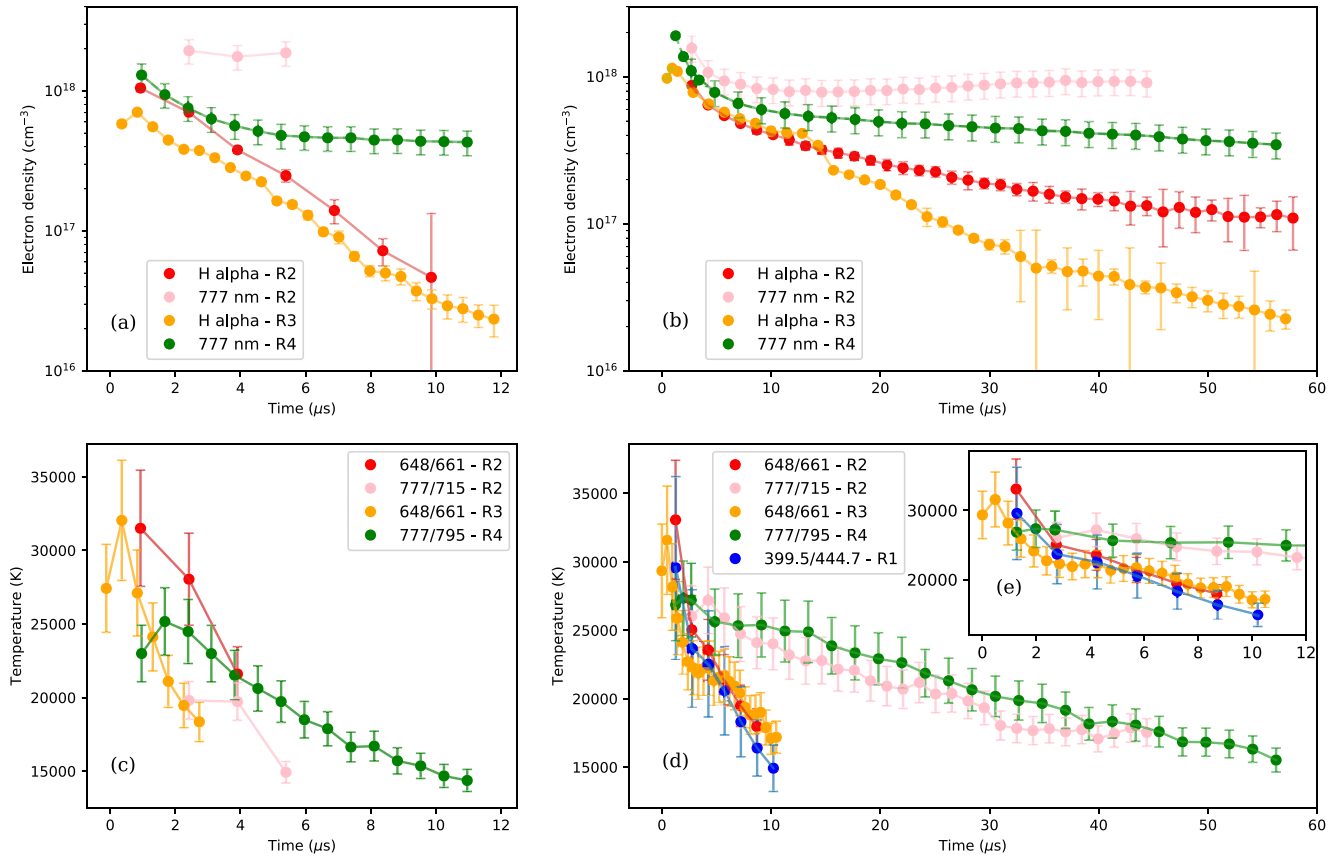


**Figure 6.** Electron densities and temperatures in a meter long lightning-like discharge produced with 800 kV in the Switching Impulse (SI) (panels [a, c] and Lightning Impulse (LI) panels [b, d]) modes. Temperatures are quantified using different combinations of neutral (O I 777 nm and O I 795 nm with R4) and ion lines (NII 648 nm and NII 661 nm with R2, and N II 399.50 nm and N II 444.70 nm with R1). Electron densities are obtained from the Stark broadening of the 777 nm O I triplet and from the full width at half area (FWHA) of the  $H_{\alpha}$  line at 656.30 nm. We have included for comparison electron densities and temperatures reported in a previous paper (see yellowish line) using grism R3 (645–665 nm) recorded at 2.1 Mfps for the same discharge and setup (Kieu et al., 2020). Note that the inset marked with (e) in panel (d) is a zoom out of the first time steps (up to 12  $\mu$ s) in panel (d).

independent of assumptions on the equilibrium state of the plasma. Consequently, electron densities are usually derived from the full width at half maximum (FWHM) of a line profile. However, it is well known that ion dynamics affects both the line widths and their shapes. This effect is especially important for the  $H_{\alpha}$  and  $H_{\gamma}$  lines, but it is nearly negligible for the line  $H_{\beta}$  (Gigosos et al., 2003). Therefore, Gigosos et al. (2003) suggested an alternative method to calculate the electron density from the Stark broadening of the  $H_{\alpha}$  line using the full width at half area (FWHA) of the  $H_{\alpha}$  with the equation:

$$N_e = 10^{17} \times \left( \frac{\text{FWHA}}{1.098} \right)^{1.47135} \text{ cm}^{-3}. \quad (1)$$

Electron densities obtained from the FWHA of the Stark broadened  $H_{\alpha}$  line in the visible-near infrared spectra (using grism R2) recorded at 672,000 fps are shown in Figures 6a and 6b (see red line) for ~1-m-long sparks in the SI and LI modes, respectively. For comparison, electron densities derived from short spectral range (using grism R3) recorded at 2,100,000 fps are also shown in Figures 6a and 6b (see yellowish dots and line). Even though our electron densities are obtained from lightning-like discharges, the results are similar to those derived by Orville (1968b) in real lightning.

For comparison with the FWHA method, the FWHM of a Stark broadened line can also be used to estimate the concentration of electrons. Griem (1964) provided a convenient equation (see below) to derive electron densities from the Stark FWHM broadening of spectral lines corresponding to neutral or singly ionized atoms:

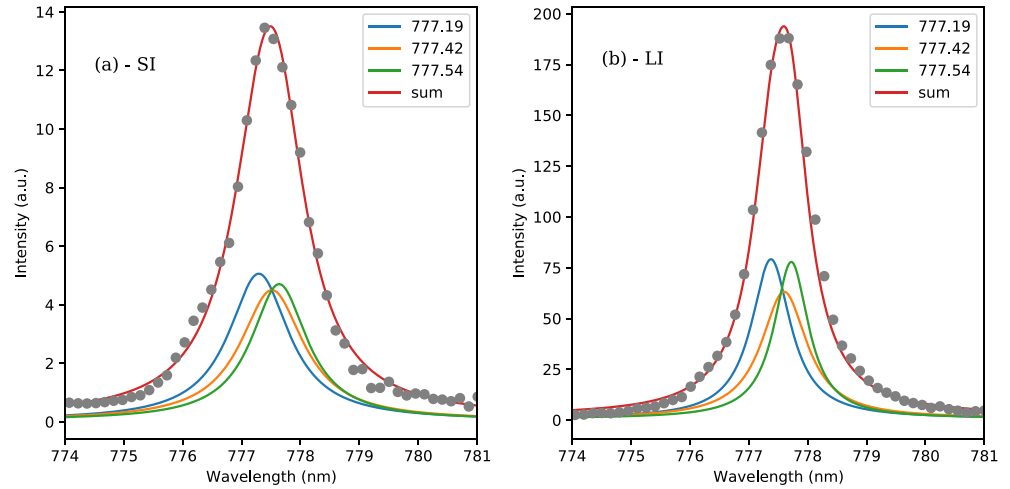


**Figure 7.** Lorentzian fit of the OI 777 nm triplet in the Switching Impulse (SI) mode (a) at  $0.964 \mu\text{s}$  and in the Lightning Impulse (LI) mode (b) at  $4.12 \mu\text{s}$  recorded with grism R4 ( $\sim 0.34 \text{ nm}$  spectral resolution). The red line is the triplet Lorentzian fit (sum) to the measured (gray dots) intensity of the O I 777 nm triplet. The blue, orange and green lines are the resulting single Lorentzians fits for each line component of the O I 777 nm triplet.

$$\Delta\lambda_{\text{Stark}}[\text{\AA}] \approx 2\omega(T) \frac{n_e[\text{cm}^{-3}]}{10^{16}}, \quad (2)$$

where  $\omega(T)$  is a tabulated function (in units of  $\text{\AA}$ ) that depends on the temperature and on the line transition wavelength considered. Equation 2 is only valid for electron densities in the range  $10^{16}$ – $10^{18} \text{ cm}^{-3}$  and it provides values of the electron density with an error within 20%–30%. Griem's calculation for  $\omega(T)$  only considered the broadening of the 777.19 nm, the strongest subline in the 777 triplet. For this subline  $\omega(T)$  varies between  $1.99 \times 10^{-2} \text{ \AA}$  at 2,500 K and  $5.56 \times 10^{-2} \text{ \AA}$  at 40,000 K Griem (1964). To make the calculation more precise, we interpolated the tabulated function  $\omega(T)$  and measured the  $\Delta\lambda_{\text{Stark}}$  of the 777.19 nm subline extracted from the full Stark broadening of the triplet. To find out the FWHM of each subline belonging to the triplet 777 nm, we built a triplet Lorentzian function ( $L_3$ ) to fit the experimental data. Since the O I 777 nm triplet is the combination of sublines 777.19, 777.41, and 777.53 nm with relative intensities 870, 810, and 750 Kramida et al. (2020), the Lorentzian function (with six fitting parameters) for the 777 nm triplet line can be written as:

$$L_3 = k + \frac{870}{810} \times \frac{I}{\pi} \frac{\sigma_1}{(\lambda - \lambda_c + a)^2 + \sigma_1^2} + \frac{I}{\pi} \frac{\sigma_2}{(\lambda - \lambda_c)^2 + \sigma_2^2} + \frac{750}{810} \times \frac{I}{\pi} \frac{\sigma_3}{(\lambda - \lambda_c - b)^2 + \sigma_3^2} \quad (3)$$

where  $k$ ,  $I$ ,  $\lambda_c$  and  $\sigma_1$ ,  $\sigma_2$ ,  $\sigma_3$  are the background of the fitting, the intensity and wavelength of the central subline of the triplet, and the broadenings of the sublines 777.19, 777.41, and 777.53 nm, respectively. The numerical values  $a = 0.223$  and  $b = 0.122$  are the shifts of the lateral wavelengths with respect to the central line of the triplet.

Figure 7 shows the resulting Lorentzian fit of the triplet 777 nm for spectra recorded with grism R4 in the Switching mode (a) at  $0.964 \mu\text{s}$  and in the Lightning mode (b) at  $4.12 \mu\text{s}$ . The fitting coefficients in the SI and LI modes for  $k$ ,  $\lambda_c$ ,  $I$ ,  $\sigma_1$ ,  $\sigma_2$ , and  $\sigma_3$  are 0.13, 777.50 nm, 9.15, 0.62, 0.65, 0.58, and 2, 777.60 nm, 100, 0.405, 0.474, 0.356. The resulting central wavelengths (777.50 and 777.60 nm) are not exactly 777.41 nm because of slight wavelength calibration detuning during the SI and LI mode spectral recording.

The electron densities obtained from the Stark broadening of the 777.19 nm subline of the O I 777 nm triplet for spectra recorded with gratings R4 and R2 are shown in Figures 6a and 6b (see green and pink lines for R4 and R2, respectively) for the SI and LI modes of a  $\sim 1$ -m-long spark produced with a peak voltage of 800 kV. We see that the maximum electron density derived from the 777.19 nm always stays above the one obtained from the  $\text{H}_\alpha$  spectral line (656.30 nm) and it seems to flatten at later times ( $\sim 4 \mu\text{s}$  and  $\sim 10 \mu\text{s}$  for the SI and

LI modes, respectively). This might be due to the fact that the FWHM method is less sensitive when the broadening of the line is not sufficiently large. We conclude that the analysis of the FWHM could be used as a first rough estimate of the electron density. The FWHA under the Stark broadened  $H_{\alpha}$  line seems to be more sensitive (than the FWHM) to the time dynamics of the electron concentration within the heated channel.

#### 4.2. Temperature

The most common method to determine the temperature of a hot plasma channel is to measure the relative intensities of different spectral lines of the same species. To calculate the gas temperature from the time resolved spectra of lightning-like discharges recorded in this work, we will assume the criteria previously established by Prueitt (1963) and Uman (1969), and also recently used by Walker and Christian (2019) for deriving the gas temperature in triggered lightning. In particular, we consider that (a) the channel of the lightning-like discharge is optically thin (there is no light absorption through the line of sight), (b) the temperature is relatively uniform along the lightning-like channel radial cross section (temperatures are similar at the edge and the center of the lightning channel), and (c) that thermal equilibrium controls the concentration of the different atoms and ion energy levels emitting light due to spontaneous radiative deexcitation, that is, the density of excited atoms and ions follow Boltzmann's law. We also assume that local thermal equilibrium (LTE) applies so that the derived electron temperature equals the gas temperature.

Therefore, the gas temperature is calculated from the intensity ratio of different pairs of lines depending on the grism used and assuming that the corresponding emitting energy levels are populated following Boltzmann's equilibrium law. In particular, for the near-ultraviolet blue spectra recorded with grism R1, we used two singly ionized nitrogen lines at 399.5 and 444.7 nm. For visible-near infrared spectra recorded with grism R2 we used the pair of lines at 648 and 661 nm associated with singly ionized nitrogen, and the pair of O I neutral lines 715 and 777 nm. Details of these calculations can be found in Kieu et al. (2020). Finally, for spectra recorded with grism R4 in the near-infrared the temperature was calculated from the ratio of the line intensities of the triplets 777 and 795 nm.

The estimation of the error in the electron temperature is evaluated with equation (11) in Walker and Christian (2019) that depends on the uncertainties in the intensity ratio and assuming a 10% uncertainty in the tabulated Einstein coefficients (Kramida et al., 2020). The uncertainty in the intensity ratio is calculated using the bootstrap method also adopted to quantify the error in the electron density.

Figures 6c and 6d show the temperatures for, respectively, the meter-long SI (Figure 6c) and LI (Figure 6d) discharges. The use of the pair of ionic lines 648 and 661 nm provide consistent temperature values with each other when used with spectra obtained with grisms R2 and R3, recorded at 672 kfps and 2.1 Mfps, respectively. The pair of N II ion lines 399.5 and 444.7 nm in the spectra recorded at 672 kfps with grism R1 (only for LI discharges) also provide consistent temperature values with those derived with grisms R2 and R3. The temperatures measured with ion lines can only be tracked for relatively short times between 2 and 4  $\mu$ s (SI mode) and up to  $\sim$ 10  $\mu$ s (LI mode). However, when neutral lines (O I 777 and 795 nm, or O I 777 and 715 nm) are employed the obtained temperatures are slightly lower (maximum of  $\sim$ 28,000 K) than the ones obtained when with ion lines (maximum of  $\sim$ 33,000 K) but can be tracked for longer times (than with ion lines) between  $\sim$ 11  $\mu$ s (SI mode) and  $\sim$ 50–60  $\mu$ s (LI mode) since neutral lines last longer. These results resemble those derived from 5-m-long lightning-like discharges in air produced with 6.4 MV by Orville et al. (1967), where it was mentioned that the ion radiation is mostly emitted from the hotter region of the channel while the neutral radiation is emitted from the cooler regions. Finally, it should be noticed that, since the 715 nm line of O I is weaker than the 795 nm line of O I, the derived temperature can be followed for shorter times when evaluated from R2 spectra (compared to R4 spectra that include the O I line at 795 nm).

#### 4.3. Time Dynamics of the Electrical Conductivity

Once the electron concentration and gas temperature are known, we can estimate the variation in time of the electrical conductivity in the heated (and highly ionized) lightning-like channel. We assume isotropic collisions so that the momentum transfer cross section  $\sigma_{tr} = \sigma_c$ , with  $\sigma_c$  being the cross section for

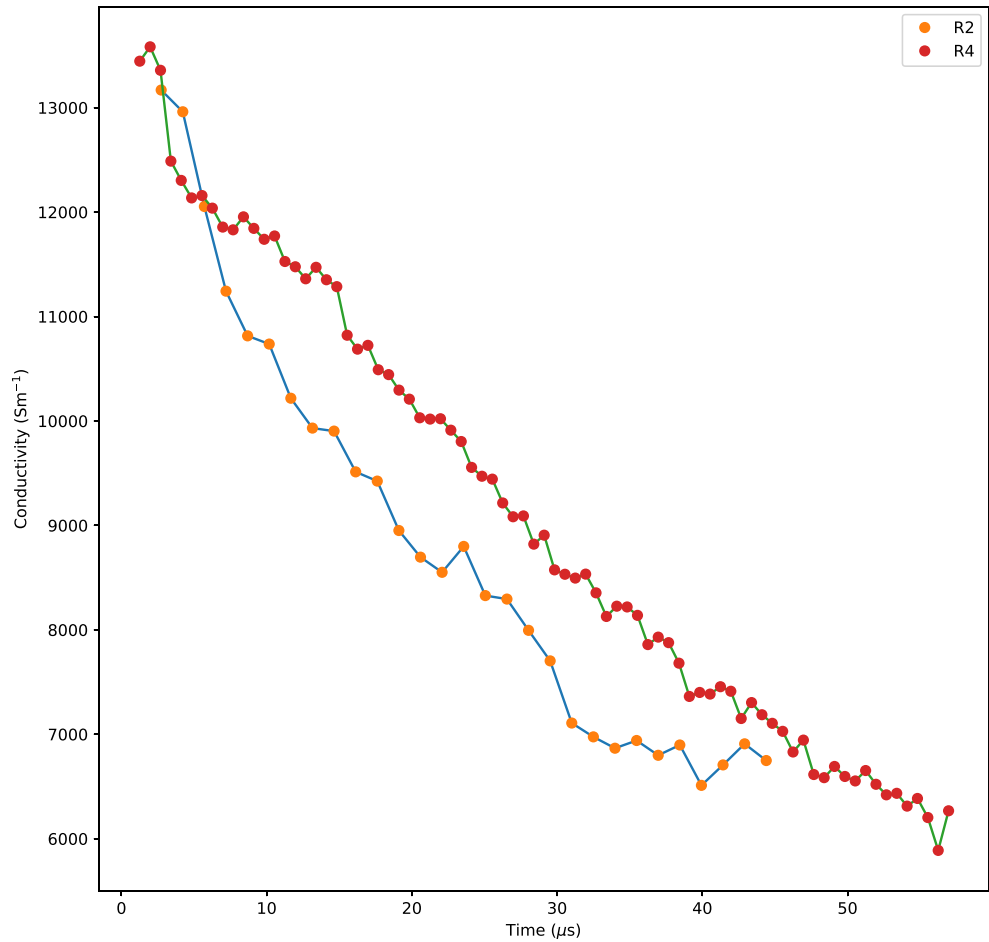


**Figure 8.** Time evolution of the electrical conductivity of a point in a heated  $\sim 1$ -m-long lightning-like discharge channel produced with 800 kV in the Lightning Impulse (LI) mode. The electrical conductivity was computed using values of  $N_e$  (see Figure 6b) and  $T$  (see Figure 6d) derived from the FWHM of the O I 777.4 nm line, and the O I line ratios 777/715 and 777/795 obtained from spectra recorded with grisms R2 and R4, respectively. The solid lines are a guide for the eye.

electron-neutral collisions. Since the heated channel is highly ionized ( $N_e/N \geq 10^{-3}$ ), it is reasonable to assume that the ion ( $N_i$ ) and electron ( $N_e$ ) densities are similar ( $N_i = N_e$ ) and, consequently, the effective collision frequency for momentum transfer  $\nu_m = N\nu\sigma_{tr} + N_e\nu\sigma_{Coulomb} \approx N_e\nu\sigma_{Coulomb}$ , where  $N$  is the gas density,  $\nu$  is the mean thermal velocity of electrons, and  $\sigma_{Coulomb}$  is the cross section of electron-ion collisions dominated by Coulomb forces. For instance, for electron (and gas) temperatures ( $T_e = T$ )  $\sim 1$  eV (11,600 K) and  $N_e = 10^{13}$  cm $^{-3}$ ,  $\sigma_{Coulomb} \approx 2 \times 10^{-13}$  cm $^2$ , while  $\sigma_{tr} \approx 10^{-16}$ – $10^{-15}$  cm $^2$  (Raizer, 1991). Thus, we can consider that the electrical conductivity  $\sigma$  in the heated lightning-like channel is controlled by  $\sigma_{Coulomb}$  as  $\sigma = e^2 N_e / m \nu_m =$  (with  $e$  and  $m$  being the electron charge and mass, respectively)  $= 1.9 \times 10^4 \times T_e(\text{eV})^{1.5}$  (ln $\Lambda$ ) $^{-1}$  S m $^{-1}$  with ln $\Lambda = 13.57 + 1.5 \log(T_e(\text{eV})) - 0.5 \log(N_e(\text{cm}^{-3}))$  (Raizer, 1991). According to Figure 8, the electrical conductivity decreases from  $1.35 \times 10^4$  S m $^{-1}$  to  $6 \times 10^3$  S m $^{-1}$  (approximately a factor of two) in  $\sim 50$   $\mu$ s mostly following the decay time scale of the temperature (see Figure 6d) from  $\sim 27,000$  K to  $\sim 15,000$  K. This indicates that high current flows are only favored in the very early times of a cloud-to-ground lightning stroke. The conductivity values obtained in this study are slightly smaller than those previously reported ( $\sim 1.6$ – $2.2 \times 10^4$  S m $^{-1}$ ) using non-time resolved lightning spectra of cloud-to-ground strokes (Guo et al., 2009). Interestingly, our conductivity values are higher and close to those recently reported in stepped leader tips ( $\sim 4.3 \times 10^3$  S m $^{-1}$ ) and dart stepped leaders ( $\sim 1.1 \times 10^4$  S m $^{-1}$ ), respectively, where, by using 20  $\mu$ s slit-less spectroscopy, the measured electron densities and gas temperatures were  $\sim 10^{15}$  cm $^{-3}$  (stepped

leader tip),  $\sim 10^{17} \text{ cm}^{-3}$  (dart-stepped leader) and  $\sim 15,000 \text{ K}$  (stepped leader tip) and  $\sim 22,000 \text{ K}$  (stepped dart leader) (Zhang et al., 2020).

## 5. Conclusions

In this study, we reported on high-speed time-resolved spectroscopic analysis of lightning-like discharges recorded by a fast and very sensitive spectrograph named GALIUS. The spectra were recorded in three separate spectral regions: near-ultraviolet blue (380–450 nm), visible near-infrared (475–793 nm), and near-infrared (770–805 nm). GALIUS spectra in the near-ultraviolet blue range, recorded at 672,000 fps (time resolution 1.488  $\mu\text{s}$ ), exhibited early time optical emissions associated to singly ionized nitrogen, oxygen, doubly ionized nitrogen, and several molecular species. In addition to the spectral features of the CN violet transition,  $\text{N}_2$  second positive system and  $\text{N}_2^+$  FNS reported in some previous studies, we found spectroscopic signatures of optical emissions due to the Swan band (516.5 nm) of  $\text{C}_2$  and of several electronically excited states of CO. These molecular species could exist in the mild temperature regions of lightning-like plasma channels and/or could be produced due to the chemical activity of streamers surrounding a heated lightning channel. Spectra in the visible-near infrared range (475–793 nm) exhibited the strongest optical emission from singly ionized nitrogen 500 N II lasting from the onset of the discharge to about 10  $\mu\text{s}$ .

Molecular species such as CN and  $\text{N}_2$  were found in high-temperature (6,000–7,000 K) combustion environments accompanied with nitrogen oxide (NO) optical emissions in the 140–340 nm spectral range (Hornkohl et al., 2014). While the 140–340 nm spectral gap is presently outside the detection range of GALIUS, our detection of molecular emissions in lightning-like channels opens the door to detect and quantify NO production by lightning using high sensitivity spectroscopic techniques. We speculate that the sensitivity of the sensor can play a key role in determining the presence of molecular species in lightning spectra.

The spectra recorded in the near infrared at 1,400,000 fps (time resolution 0.714  $\mu\text{s}$ ) showed the dynamics of two distinct O I triplets at 777 and 795 nm. Optical emissions from the 777 nm triplet, which are the strongest ones, begin almost at the onset of the discharge at about 0.25–0.55  $\mu\text{s}$  and last up to  $\sim 100 \mu\text{s}$  following the input current. These O I triplets and the O I 715 nm line were used to calculate the gas temperature inside the lightning-like channel. The gas temperature was also evaluated from the ratio of two pairs of N II ion lines (648 and 661 nm, and 399.5 and 444.7 nm) and compared with the temperature derived from pairs of neutral O I lines. The temporal dynamic of the gas temperatures is conditioned by the lifetime of ion and neutrals lines. Thus, while the final temperatures are roughly the same ( $\sim 15,000 \text{ K}$ ) for the LI mode, ionic lines can provide more reliable temperatures in the early times ( $\leq 2 \mu\text{s}$ ) but neutrals can be followed longer and can better account for the thermal relaxation of the lightning-like channel.

We have completed our measurements with simulated spectra. The comparison between measured and synthetic spectra reveal some disagreements that could be due to inaccuracies of available spectroscopic constants, calculated Stark broadening mechanisms and/or underlying model approximations (equilibrium assumptions).

Finally, the concentration of electrons within the heated channel was determined by the analysis of the Stark broadening of spectral lines. We compared the electron densities resulting from the FWHM under the  $\text{H}_\alpha$  line, and from the FWHM of the neutral 777.19 nm O I line. For the  $\text{H}_\alpha$  broadening, electron densities were in a good agreement with those obtained in real lightning (Orville, 1968b) but the estimations from the FWHM of the 777.19 nm overestimated electron number concentrations and can be considered as a rough estimation.

## Data Availability Statement

The spectroscopic data (processed data and source python scripts used for figure generation) presented in this article are available through figshare (<https://cutt.ly/zcRpNzK>).

**Acknowledgments**

This work has received funding from the European Union Horizon 2020 research and innovation program under the Marie Skłodowska-Curie grant agreement SAINT 722337. Additionally, this work was supported by the Ministerio de Ciencia e Innovación-Agencia Estatal de Investigación, under project PID2019-109269RB-C43 and FEDER program. F. J. Pérez-Invernón acknowledges the sponsorship provided by the Federal Ministry for Education and Research of Germany through the Alexander von Humboldt Foundation. T. N. K. F. J. Gordillo-Vázquez, M. Passas, and J. Sánchez acknowledge financial support from the State Agency for Research of the Spanish MCIU through the “Center of Excellence Severo Ochoa” award for the Instituto de Astrofísica de Andalucía (SEV-2017-0709). The authors acknowledge Prof. J. Montanya (of UPC) and LABLEC for having granted access to high voltage facilities in Terrassa (Spain).

**References**

Al-Tuwirqi, R., Al-Suliman, N., Khalil, A., & Gondal, M. (2012). New observation of the quintet states of CO excited by glow discharge. *Molecular Physics*, *110*, 2951–2956. <https://doi.org/10.1080/00268976.2012.686640>

Bekefi, G. (1976). *Principles of laser plasmas*. New York: Wiley.

Camacho, J., Poyato, J., Diaz, L., & Santos, M. (2007). Optical emission studies of nitrogen plasma generated by IR CO<sub>2</sub> laser pulses. *Journal of Physics B: Atomic, Molecular and Optical Physics*, *40*, 4573–4590. <https://doi.org/10.1088/0953-4075/40/24/003>

Carbone, E., D’Isa, F., Hecimovic, A., & Fantz, U. (2020). Analysis of the C<sub>2</sub> Swan bands as a thermometric probe in CO<sub>2</sub> microwave plasmas. *Plasma Sources Science and Technology*, *29*, 055003. <https://doi.org/10.1088/1361-6595/ab74b4>

Cho, M., & Rycroft, M. J. (1998). Computer simulation of the electric field structure and optical emission from cloud-top to the ionosphere. *Journal of Atmospheric and Solar-Terrestrial Physics*, *60*, 871–888. [https://doi.org/10.1016/s1364-6826\(98\)00017-0](https://doi.org/10.1016/s1364-6826(98)00017-0)

Crispim, L., Peters, F., Amorim, J., Hallak, P., & Ballester, M. (2021). On the CN production through a spark-plug discharge in air-CO<sub>2</sub> mixture. *Combustion and Flame*, *226*, 156–162. <https://doi.org/10.1016/j.combustflame.2020.11.043>

Cummer, S. A., & Füllekrug, M. (2001). Unusually intense continuing current in lightning produces delayed mesospheric breakdown. *Geophysical Research Letters*, *28*, 495–498. <https://doi.org/10.1029/2000gl012214>

Cummer, S. A., Frey, H. U., Mende, S. B., Hsu, R.-R., Su, H.-T., Chen, A. B., & Takahashi, Y. (2006). Simultaneous radio and satellite optical measurements of high-altitude sprite current and lightning continuing current. *Journal of Geophysical Research*, *111*. <https://doi.org/10.1029/2006ja011809>

Czech, T., Sobczyk, A., Jaworek, A., & Krupa, A. (2012). Corona and back discharges in flue-gas simulating mixture. *Journal of Electrostatics*, *70*, 269–284. <https://doi.org/10.1016/j.elstat.2012.03.005>

Czech, T., Sobczyk, A., Jaworek, A., Krupa, A., & Rajch, E. (2013). Studies of corona and back discharges in carbon dioxide. *The European Physical Journal D*, *67*, 23. <https://doi.org/10.1140/epjd/e2012-30572-7>

Dong, M., Chan, G. C.-Y., Mao, X., Gonzalez, J., Lu, J., & Russo, R. (2014). Elucidation of C<sub>2</sub> and CN formation mechanisms in laser-induced plasmas through correlation analysis of carbon isotopic ratio. *Spectrochimica Acta Part B: Atomic Spectroscopy*, *100*, 62–69. <https://doi.org/10.1016/j.sab.2014.08.009>

Fisher, R., Schnetzer, G., Thottappillil, R., Rakov, V., Uman, M., & Goldberg, J. (1993). Parameters of triggered-lightning flashes in florida and alabama. *Journal of Geophysical Research*, *98*, 22887–22902. <https://doi.org/10.1029/93jd02293>

Gigosos, M., González, M., & Cardeñoso, V. (2003). Computer simulated Balmer-alpha, beta and gamma Stark line profiles for non-equilibrium plasmas diagnostics. *Spectrochimica Acta Part B: Atomic Spectroscopy*, *58*, 1489–1504. [https://doi.org/10.1016/s0584-8547\(03\)00097-1](https://doi.org/10.1016/s0584-8547(03)00097-1)

Gilmore, F. R., Laher, R. R., & Espy, P. J. (1992). Franck-Condon factors, r-centroids, electronic transition moments, and Einstein coefficients for many nitrogen and oxygen band systems. *Journal of Physical and Chemical Reference Data*, *21*, 1005–1107. <https://doi.org/10.1063/1.555910>

Gordillo-Vázquez, F. J., Luque, A., & Simek, M. (2012). Near infrared and ultraviolet spectra of TLEs. *Journal of Geophysical Research*, *117*, A05329. <https://doi.org/10.1029/2012ja017516>

Gordillo-Vázquez, F. J., Passas, M., Luque, A., Sánchez, J., Velde, O., & Montanyá, J. (2018). High spectral resolution spectroscopy of sprites: A natural probe of the mesosphere. *Journal of Geophysical Research: Atmospheres*, *123*, 2336–2346. <https://doi.org/10.1002/2017jd028126>

Gordillo-Vázquez, F. J., & Pérez-Invernón, F. (2021). A review of the impact of transient luminous events on the atmospheric chemistry: Past, present, and future. *Atmospheric Research*, *252*, 105432. <https://doi.org/10.1016/j.atmosres.2020.105432>

Gordillo-Vázquez, F. J., Pérez-Invernón, F. J., Huntrieser, H., & Smith, A. K. (2019). Comparison of six lightning parameterizations in CAM5 and the impact on global atmospheric chemistry. *Earth and Space Science*, *6*, 2317–2346. <https://doi.org/10.1029/2019EA000873>

Griem, H. (1964). *Plasma spectroscopy*. New York: McGraw-Hill.

Guo, Y.-X., Yuan, P., Shen, X.-Z., & Wang, J. (2009). The electrical conductivity of a cloud-to-ground lightning discharge channel. *Physica Scripta*, *80*, 035901. <https://doi.org/10.1088/0031-8949/80/03/035901>

Hampton, D. L., Heavner, M. J., Wescott, E. M., & Sentman, D. D. (1996). Optical spectral characteristics of sprites. *Geophysical Research Letters*, *23*, 89–92. <https://doi.org/10.1029/95GL03587>

Hornkohl, J., Fleischmann, J., Surmick, D., Witte, M., Swafford, L., Woods, A., & Parigger, C. (2014). Emission spectroscopy of nitric oxide in laser-induced plasma. *Journal of Physics: Conference Series*, *548*, 012040. <https://doi.org/10.1088/1742-6596/548/1/012040>

Kanmae, T., Stenbaek-Nielsen, H. C., & McHarg, M. G. (2007). Altitude resolved sprite spectra with 3 ms temporal resolution. *Geophysical Research Letters*, *34*, L07810. <https://doi.org/10.1029/2006GL028608>

Kieu, N., Gordillo-Vázquez, F. J., Passas, M., Sánchez, J., Pérez-Invernón, F. J., Luque, A., & Christian, H. (2020). Sub-microsecond spectroscopy of lightning-like discharges: Exploring new time regimes. *Geophysical Research Letters*, *47*, e2020GL088755. <https://doi.org/10.1029/2020GL088755>

Kolmašová, I., Santolík, O., Kašpar, P., Popek, M., Pizzuti, A., Spurný, P., et al. (2021). First observations of elves and their causative very strong lightning discharges in an unusual small-scale continental spring-time thunderstorm. *Journal of Geophysical Research: Atmospheres*, *126*, e2020JD032825. <https://doi.org/10.1029/2020JD032825>

Kramida, A., Ralchenko, Y., & Reader, J., & NIST ASD Team. (2020). *NIST atomic spectra database*. Gaithersburg, MD: National Institute of Standards and Technology. Retrieved from <https://physics.nist.gov/asd>

Levine, J. S., Hughes, R. E., Chameides, W. L., & Howell, W. E. (1979). N<sub>2</sub>O and CO production by electric discharge: Atmospheric implications. *Geophysical Research Letters*, *6*, 557–559. <https://doi.org/10.1029/gl006i007p00557>

Little, C., & Browne, P. (1987). Origin of the high-pressure bands of C<sub>2</sub>. *Chemical Physics Letters*, *134*, 560–564. [https://doi.org/10.1016/0009-2614\(87\)87193-2](https://doi.org/10.1016/0009-2614(87)87193-2)

Luque, A., & Gordillo-Vázquez, F. J. (2011). Modeling and analysis of N<sub>2</sub>(B<sup>3</sup>Π<sub>g</sub>) and N<sub>2</sub>(C<sup>3</sup>Π<sub>u</sub>) vibrational distributions in sprites. *Journal of Geophysical Research: Space Physics*, *116*. <https://doi.org/10.1029/2010ja015952>

Luque, A., Gordillo-Vázquez, F. J., Li, D., Malagón-Romero, A., Pérez-Invernón, F. J., Schmalzried, A., et al. (2020). Modeling lightning observations from space-based platforms (cloudscat. jl 1.0). *Geoscientific Model Development*, *13*, 5549–5566. <https://doi.org/10.5194/gmd-13-5549-2020>

Murray, L. T. (2016). Lightning NO<sub>x</sub> and impacts on air quality. *Current Pollution Reports*, *2*, 115–133. <https://doi.org/10.1007/s40726-016-0031-7>

Newman, M., Stahmann, J., Robb, J., Lewis, E., Martin, S., & Zinn, S. (1967). Triggered lightning strokes at very close range. *Journal of Geophysical Research*, *72*, 4761–4764. <https://doi.org/10.1029/jz072i018p04761>

- Orville, R. (1968a). A high-speed time-resolved spectroscopic study of the lightning return stroke: Part I. A qualitative analysis. *Journal of the Atmospheric Sciences*, 25, 827–838. [https://doi.org/10.1175/1520-0469\(1968\)025<0827:ahstrs>2.0.co;2](https://doi.org/10.1175/1520-0469(1968)025<0827:ahstrs>2.0.co;2)
- Orville, R. (1968b). A high-speed time-resolved spectroscopic study of the lightning return stroke: Part II. A quantitative analysis. *Journal of the Atmospheric Sciences*, 25, 839–851. [https://doi.org/10.1175/1520-0469\(1968\)025<0839:ahstrs>2.0.co;2](https://doi.org/10.1175/1520-0469(1968)025<0839:ahstrs>2.0.co;2)
- Orville, R., & Uman, M. (1965). The optical continuum of lightning. *Journal of Geophysical Research*, 70, 279–282. <https://doi.org/10.1029/jz070i002p00279>
- Orville, R., Uman, M., & Sletten, A. (1967). Temperature and electron density in long air sparks. *Journal of Applied Physics*, 38, 895–896. <https://doi.org/10.1063/1.1709443>
- Parra-Rojas, F. C., Luque, A., & Gordillo-Vázquez, F. J. (2015). Chemical and thermal impact of sprite streamers in the Earth mesosphere. *Journal of Geophysical Research: Space Physics*, 120, 8899–8933. <https://doi.org/10.1002/2014JA020933>
- Parra-Rojas, F. C., Passas, M., Carrasco, E., Luque, A., Tanarro, I., Simek, M., & Gordillo-Vázquez, F. J. (2013). Spectroscopic diagnosis of laboratory air plasmas as a benchmark for spectral diagnosis of TLEs. *Journal of Geophysical Research*, 118, 4649–4661. <https://doi.org/10.1002/jgra.50433>
- Passas, M., Sánchez, J., Kieu, T., Sánchez-Blanco, E., & Gordillo-Vázquez, F. J. (2019). GALIUS: An ultrafast imaging spectrograph for the study of lightning. *Applied Optics*, 58, 8002–8006. <https://doi.org/10.1364/ao.58.008002>
- Passas, M., Sánchez, J., Sánchez-Blanco, E., Luque, A., & Gordillo-Vázquez, F. J. (2016). GRASSP: A spectrograph for the study of transient luminous events. *Applied Optics*, 55, 6436–6442. <https://doi.org/10.1364/AO.55.006436>
- Pérez-Invernón, F. J., Luque, A., & Gordillo-Vázquez, F. J. (2018). Modeling the chemical impact and the optical emissions produced by lightning-induced electromagnetic fields in the upper atmosphere: The case of halos and elves triggered by different lightning discharges. *Journal of Geophysical Research: Atmospheres*, 123, 7615–7641.
- Prueitt, M. (1963). The excitation temperature of lightning. *Journal of Geophysical Research*, 68, 803–811. <https://doi.org/10.1029/jz068i003p00803>
- Raizer, Y. P. (1991). *Gas discharge physics. Fizika gazovogo razryada*. Berlin: Springer.
- Ripoll, J.-F., Zinn, J., Jeffery, C. A., & Colestock, P. L. (2014). On the dynamics of hot air plasmas related to lightning discharges: 1. Gas dynamics. *Journal of Geophysical Research: Atmospheres*, 119, 9196–9217. <https://doi.org/10.1002/2013jd020067>
- Salanave, L. (1961). The optical spectrum of lightning. *Science*, 134, 1395–1399. <https://doi.org/10.1126/science.134.3488.1395>
- Salanave, L., Orville, R., & Richards, C. (1962). Slitless spectra of lightning in the region from 3850 to 6900 angstroms. *Journal of Geophysical Research*, 67, 1877–1884. <https://doi.org/10.1029/jz067i005p01877>
- Soler, S., Pérez-Invernón, F. J., Gordillo-Vázquez, F., Luque, A., Li, D., Malagón-Romero, A., et al. (2020). Blue optical observations of narrow bipolar events by ASIM suggest corona streamer activity in thunderstorms. *Journal of Geophysical Research: Atmospheres*, 125, e2020JD032708. <https://doi.org/10.1029/2020jd032708>
- Uman, M. (1963). The continuum spectrum of lightning. *Journal of Atmospheric and Terrestrial Physics*, 25, 287–295. [https://doi.org/10.1016/0021-9169\(63\)90025-4](https://doi.org/10.1016/0021-9169(63)90025-4)
- Uman, M. (1964). The peak temperature of lightning. *Journal of Atmospheric and Terrestrial Physics*, 26, 123–128. [https://doi.org/10.1016/0021-9169\(64\)90113-8](https://doi.org/10.1016/0021-9169(64)90113-8)
- Uman, M. A. (1969). Determination of lightning temperature. *Journal of Geophysical Research*, 74, 949–957. <https://doi.org/10.1029/jb074i004p00949>
- Uman, M., & Orville, R. (1964). Electron density measurement in lightning from stark-broadening of H<sub>α</sub>. *Journal of Geophysical Research*, 69, 5151–5154. <https://doi.org/10.1029/jz069i024p05151>
- Uman, M., & Orville, R. (1965). The opacity of lightning. *Journal of Geophysical Research*, 70, 5491–5497. <https://doi.org/10.1029/jz070i022p05491>
- Uman, M., Orville, R., & Salanave, L. (1964). The density, pressure, and particle distribution in a lightning stroke near peak temperature. *Journal of the Atmospheric Sciences*, 21, 306–310. [https://doi.org/10.1175/1520-0469\(1964\)021<0306:tdpapd>2.0.co;2](https://doi.org/10.1175/1520-0469(1964)021<0306:tdpapd>2.0.co;2)
- Walker, T., & Christian, H. (2017). Triggered lightning spectroscopy: Part 1. A qualitative analysis. *Journal of Geophysical Research: Atmospheres*, 122, 8000–8011. <https://doi.org/10.1002/2016jd026419>
- Walker, T., & Christian, H. (2019). Triggered lightning spectroscopy: 2. A quantitative analysis. *Journal of Geophysical Research: Atmospheres*, 124, 3930–3942. <https://doi.org/10.1029/2018jd029901>
- Wallace, L. (1960). Note on the spectrum of lightning in the region 3670 to 4280 Å. *Journal of Geophysical Research*, 65, 1211–1214. <https://doi.org/10.1029/jz065i004p01211>
- Wallace, L. (1964). The spectrum of lightning. *The Astrophysical Journal*, 139, 994. <https://doi.org/10.1086/147833>
- Zhang, N., Yuan, P., ting An, T., Zhang, M., & rong Chen, R. (2020). The conductivity and propagation property of lightning leader tip. *Atmospheric Research*, 245, 105099. <https://doi.org/10.1016/j.atmosres.2020.105099>
- Zhivlyuk, Y., & Mandel'shtam, S. (1961). On the temperature of lightning and force of thunder. *Soviet Physics JETP*, 13, 338.